Journal of Manufacturing Processes 124 (2024) 1554–1566

Contents lists available at ScienceDirect

Journal of Manufacturing Processes

journal homepage: www.elsevier.com/locate/manpro

# Determination of energies in high-speed blanking

Fabian Schmitz [a,*], Till Clausmeyer [a,b], Marlon Hahn [a], A. Erman Tekkaya [a]

[a] Institute of Forming Technology and Lightweight Components (IUL), TU Dortmund University, 44227 Dortmund, Germany
[b] Now at: Professorship Forming Technology, Chemnitz University of Technology, 09126 Chemnitz, Germany

ARTICLE INFO

*Keywords:*
High-speed blanking
Adiabatic blanking
Energy analysis in high-speed blanking
Adiabatic shear band formation
Process efficiency

ABSTRACT

High speed blanking is a process in which the speed of the punch exceeds a specific material threshold to produce localization phenomena in the blanking clearance, leading to thermal softening and eventually to a shear band formation. The analysis of the formation of these shear bands requires the analysis of the energies for the initiation of shear bands for the mechanical and thermal boundary conditions, and the knowledge of the amount of energy for maintaining the localized deformation until material separation. This paper presents an approach to determine the available process energy for a high-speed blanking process, and the energy dissipated for high carbon steel C75 and a AA5083 aluminum alloy. With these energies the material-independent efficiency of the tool (28 %) and the material-dependent efficiency of the blanking process (2.6–71.8 %) are calculated, leading to a total efficiency between 0.73 % to 20.1 %. This approach provides a basis to compare various investigations on high speed blanking. Using process forces and strain formulation, an instability criterion identifies instability points, approximating energy dissipation pre- and post-instability for blanking. It was found, that the energy required for deformation from the instant of instability until material separation increases as the tool speed increases. When ASB are formed, the evaluation of these energies shows increased energy dissipation per volume by a factor of 20 or more. For all blanking experiments a peak acceleration larger than 26,120 g was measured, revealing the dynamic nature of this impact process.

## 1. Introduction

**Table 1**
Frequently used quantities for analysis.

| Measured quantities | | Determined quantities | | |
|---|---|---|---|---|
| $a_{punch}$ | Acceleration of the punch | $\dot{\bar{\varepsilon}}$ | (Eq. 1) | Engineering strain rate |
| $A$ | Sheared area | $l_{\text{tool}}$ | (Eq. 6) | Displacement of the punch during impact |
| $c$ | Total clearance | $v^0_{\text{tool}}$ | (Eq. 5) | Speed at onset of impact |
| $c_{\%}$ | Relative clearance | $E^0_{\text{kin}}$ | (Eq. 4) | Initial kinetic punch energy |
| $F_{\text{shear}}$ | Shear force during impact | $E_{\text{shear}}$ | (Eq. 7) | Shear energy |
| $m_{\text{tool}}$ | Mass of the tool | $\varepsilon_{\max}$ | (Eq. 10) | Strain at fracture |
| $t_0$ | Time at onset of impact | $\eta$ | (Eq. 8) | Efficiency of the blanking process |
| $t_1$ | Time at end of impact | | | |

Blanking is one of the most widely used processes for sheet metal, since every sheet is usually blanked once for trimming. The objective of the blanking process is to separate the coin from the skeleton. Optimally, the blanked edge is straight, exhibits a small surface roughness, and has similar material properties as the base material. Other requirements are the absence of a burr and little or no roll-over, i.e. plastic bending at the upper and lower surface of the blanked sheet. However, blanked edges are often characterized by three different surface zones: the desired straight burnish with low roughness, a fracture zone inclined to the burnish, exhibiting higher roughness, and an undesired burr. The geometrical and material properties of the blanked edge are determined by the process parameters. While usually a tool speed in the range of 0.1…1 m/s is used, blanking at higher speeds offers the opportunity to produce lower surface roughness and higher straightness of the edges [1]. At lager punch speeds, localized deformation may occur, leading to enhanced properties of blanked edges.

At increased punch speeds, the strain rate in the deformation zone increases to the range of $10^4 - 10^6\ s^{-1}$ compared to $\approx 10^3\ s^{-1}$ for conventional blanking. Materials with positive strain rate sensitivity exhibit an increase in plastic heating, due to the increased plastic work.

* Corresponding author.

https://doi.org/10.1016/j.jmapro.2024.07.028
Received 5 December 2023; Received in revised form 2 July 2024; Accepted 3 July 2024
Available online 17 July 2024

Depending on the heat conductivity of a material, the increased plastic work may lead to extensive heating and thermal softening. In materials such as steels or titanium with low conductivity, the extent of thermal softening exceeds the strain rate depending hardening and leads to localization. For simple shear Recht [2] derived a mathematical criterion for the onset of such a strain localization. In results of [3] the strain localization leads to the formation of shear bands, and eventually to straight edges with low distortion of the coin [1]. Not only the speed of the tool, but also the total energy of the active tool is a driving process quantity. Due to different concepts for acceleration (electromagnetic [4], explosion [5], combustion [6], gas springs [7]) the initial tool speed at impact and the correlated initial kinetic energy is often used for comparison. In the analysis [1] of high-speed blanking, Davies and Dhawan used pneumatic energy of their air-driven machine and the punch speed upon impact as process parameters describing their high-speed blanking experiment. The same quantities, speed and energy, were used as characterizing process parameters by Travis and Johnson [8] for their experiments. However, since the mass of the tools and the driving mechanism of the machine were different, the mentioned energies are not comparable. In particular, the machine and tool concept can vary, which reduces the quality of the comparability. Another cause of complicating comparisons might be different machine or tool efficiencies. This demonstrates the clear need to establish comparable measures of energy and efficiency for high speed blanking. An alternative measure is the amount of energy dissipated by the blanked material, which differs considerably with the kinetic energy due to different efficiencies.

In this work, first the fundamentals of blanking (Section 1.1) and the special feature of local deformation in high-speed blanking are described. Subsequently, the investigation of blanking energies (Section 1.2) focuses on the different methods and findings and contradictions in the literature on high speed blanking, a supplementation by new investigations, methods and results (Section 1.3) is incorporated.

### 1.1. Conventional and high speed blanking

In blanking a shear deformation occurs between the tools, usually by the moving punch and the fixed die (Fig. 1). The absolute clearance $c$ describes the gap between the punch and the die and is given by $c = 0.5(d_{die} - d_{tool})$ for a circular part. The clearance is a coarse measure for the size of the sheared zone and has a large effect on the properties of shear-cut edges. In [9] both an increase of the clearance or punch diameter increases the resulting burr high.

In general, larger clearances lead to a more pronounced fracture zone. When comparing results of different blanking experiments one uses the relative clearance $c_{\%} = c/s$, which normalizes the clearance by the sheet thickness $s$. The fracture zone is created during the material separation process and attributed to tensile stress states, which lead to excessive plastic strain beyond the fracture strain. For a relative clearance of 10 % the deformed zone extends beyond the area marked by the clearance, see Fig. 2. The width of the strain affected zone $w$ depends on the clearance, the material properties and the punch speed. In an early report of the positive effect of elevated punch speeds on shearing, Zener and Hollomon [11] observed a narrow shear band of martensitic layer of 31.7 µm for a punch speed of approximately $v_{tool}^{Zener} = 3$ m/s for an upsetting process.

Different measures of strain rate can be introduced to compare different blanking results. Assuming ideal, homogeneous simple shear deformation only in the region of the clearance, the equivalent engineering strain rate is defined as

$$\dot{\bar{\varepsilon}} = \frac{1}{\sqrt{3}} v_{tool}/c. \tag{1}$$

However, the small width of the localized deformation zone $w$, observed as white band by Zener and Hollomon, indicates that an estimation based on the nominal clearance is misleading. Therefore, the effective strain rate

$$\dot{\bar{\varepsilon}}_{eff} = \frac{1}{\sqrt{3}} v_{tool}/w \tag{2}$$

is introduced, now assuming ideal simple shear with the localization width $w$. The results in nominal and effective strain rate $\dot{\bar{\varepsilon}}$ are 1,875 $s^{-1}$ and 96,774 $s^{-1}$. In case of high punch speeds, the differentiation of the localized deformation zone and the surrounding base material is possible because of visible microstructural changes in light optical micrographs (see Fig. 1 and Fig. 2). In both micrographs the highly localized shear bands have a lighter color. Zener and Hollomon attribute this to martensitic formation due to heating above the austenitisation temperature during shearing. The shear strain is estimated as 100 in Fig. 2 [11]. Due to the high temperature increase occurring in a small (< 1 ms) time period allowing almost no heat conduction, Zener and Hollomon used the term “adiabatic” to refer to their shearing process. In the current work the term high-speed blanking is used to refer to the previously mentioned process, which focus at localizing strains due to high punch speeds. In contrast, blanking with punch speeds <1 m/s is referred to as conventional blanking.

In contrast to conventional blanking, Davis and Dhawan [6] observed experimentally a sheared surface exhibiting partly a very high strength, while the surrounding area was not affected by the shear deformation. This is attributed to the strain localization and leads to sheared surfaces which differ in geometry [5] and mechanical properties, like the hardness distribution [13] (Fig. 3). However, the effect of quality improvement of the surface saturates at a certain tool speed vanishes around 120 m/s [6].

### 1.2. Investigation of blanking energies

Since, the results of Davies and Dhawan [6] indicate that the

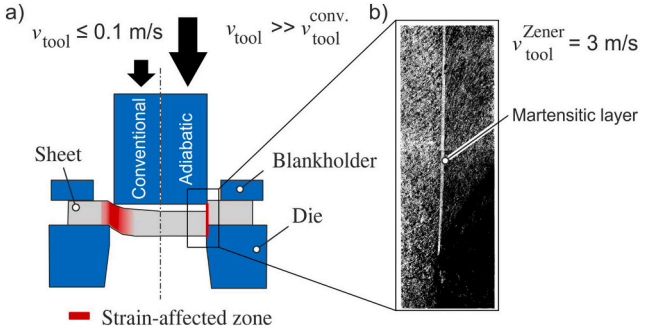


**Fig. 1.** (a) Schematic comparison of conventional and high-speed blanking [10], (b) Illustration of adiabatic shear band [11] found in blanking with a blanking speed of 3 m/s and strain rates of 2,000 1/s.

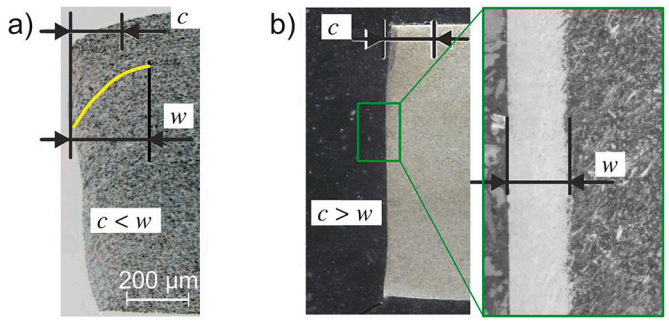


**Fig. 2.** (a) Conventional blanking: Effective strain-affected zone $w$ is larger than the blanking clearance $c$ [12], (b) high-speed blanking: Strain is localized in the clearance $c$ and w is smaller than c [10].

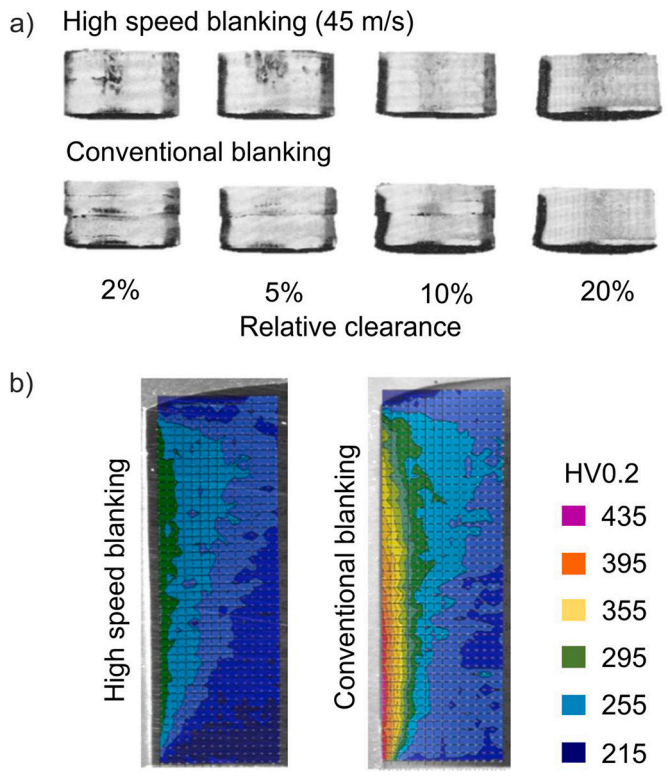


**Fig. 3.** Comparison of sheared surfaces of conventional and high speed blanking (a) Geometrical properties adapted from [5], (b) Hardness distribution adapted from [13].

variation of punch speed with an identical initial energy influences the results of high-speed blanking, a method to determine different physical energy quantities for different high-speed blanking set-ups is needed. In conventional blanking the punch is usually fixed mechanically to the crank and the ram of a servo-press or the piston of a hydraulic press. In this setting, the shear energy $E_{shear}$ can be determined by integrating the punch force $F_p$ over the punch displacement $l_{punch}$:

$$E_{shear} = \int F_p \, dl_{punch}. \tag{3}$$

However, due to the different set-up of machines used for high-speed blanking, the punch force $F_p$ cannot be measured, therefore a modified method is required. Those set-ups have in common that the punch is not fixed permanently to a drive part of the machine. Therefore, these set-ups are energy-controlled forming machines and the energy transfer to the sheared sheet is not completely determined by the machine kinematics comparable as with hammers. In addition, the vibration induced by the impact can overlap the force signal, so that interference-free measurements can only be achieved by special setups [14]. The initial kinetic energy

$$E^0_{kin} = \frac{1}{2} m v^2_{v_{tool}(t=t_0)}, \tag{4}$$

at the time of the impact $t_0$ of the punch on the sheet with the mass $m$ is introduced to analyze high-speed blanking with an energy-controlled set-up. Johnson and Travies [8] determined the tool speed by the time it takes to rupture two thin lead strips in a defined distance placed in the direction of the punch movement. For high-speed blanking Davies and Dhawan [15] tracked the displacement by a copper device, which tracks the change of an electric capacitance by the pass of the punch. The underlying assumption was a linear behavior of the correlation between displacement and change of capacitance. With his method the current speed during blanking could be obtained, but with an overlapping oscillation (Fig. 4). For successful blanking, this energy can be used as an approximation for the required energy for blanking. Johnson and Slater [16] reported an increase of the required initial kinetic energy $E^0_{kin}$ with increasing tool speeds in the range of $v_0 = 15.24$ m/s. Johnson and Travies [8] extended the analysis by investigating higher punch speeds between $v_0 = 60$–$210$ m/s and varied the initial kinetic energy $E^0_{kin}$ by the mass of the punch. Davies and Dhawan [6] found a saturation effect of the tool speed above 10–12 m/s on the associated increase of part quality in terms of straightness. In contrast to [8,16] Davies and Dhawan [6] calculated the energy for shear deformation $E_{shear}$, i.e. the process energy, by integration of the force displacement, Eq. (3), curve for various materials and punch speeds. They found that the peak force $F_{max}$ for high-speed blanking is always larger in comparison to quasi-static blanking, while the required blanking energy $E_{shear}$ differs in relation to quasi-static blanking processes (Fig. 4).

Davies and Austin [17] used (Eq. (3) to determine the shear energy for high-speed blanking $E_{high}$ and conventional blanking $E_{conv}$. Putting these values into relation ($R^{high}_{conv} = \frac{E_{high}}{E_{conv}}$) factors between $R^{high}_{conv} = 0.56\ldots 1.98$ could be determined [17]. In particular, for high carbon steel Davies and Dhawan [6] showed for lower relative blanking clearances $c_{\%}$ in the range of 2 % - 8 %, that the energy requirement in terms of $E^0_{kin}$ decreases in high-speed blanking. Despite the fact that the used high carbon steel has a lower ductility and is prone to cracking, and thus has lower energy requirements, these findings were in good correlation with the work of Zener and Hollomon. Later, Davies and Dhawan [15] validated these findings and reported that the initial kinetic energy required, $E^0_{kin}$, depends on the thickness $s$ of the sheet material. For a reduction of constant absolute clearance $c$ an increase of the required energy $E_{shear}$ for quasi-statically blanked parts was found, while for high-speed processes a drop in the energy $E_{shear}$ occurred.

### 1.3. Further aspects of high-speed blanking

While a number of investigations on the localization of strains under compression and impact loading exist, only few focus on the occurrence in processes like blanking for the last 50 years. Different newly developed setups were used to determine the influence of the process speed, but also energy converters [18] were developed to utilize conventional presses for high-speed blanking. Due to very high strengths of the workpiece materials, high-speed blanking was reconsidered by Högman et al. [19] and investigated further by Neugebauer et al. [20]. For high strength materials, a very high straightness of 90°±1° and a surface with a roughness of $R_a = 1.3$ µm were found [19], while in [21] adiabatic shear band formation for initial tool speeds of ≥7 m/s was reported, regardless of the impact energy for hardened 22MnB5 steel material. So far, in-process investigations have been limited to the determination of

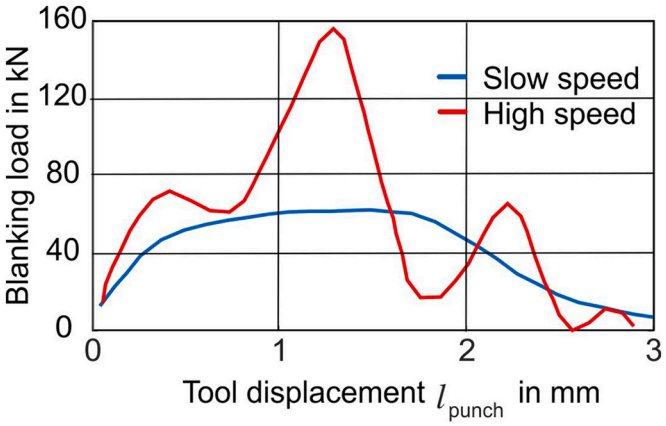


**Fig. 4.** Comparison of blanking load for high (10 m/s) and low (0.21 mm/s) tool speed for mild steel adapted from [6].

the shear-affected area for blanking [13], numerical analyses of strain localizing effects in high-speed blanking [22], semi-analytical investigations of the effect on the local softening during blanking [23] and associated local temperatures determined by experiments and simulation [24]. An investigation of conventional processes regarding the stress state in the blanking clearance was carried out by Silva et al. [25]. In their work, the stress states for conventional blanking and fine blanking were determined on the basis of an analytical model. For high-speed blanking low triaxialities $\eta^* \leq 0$ [10] were found, which can also be found in fine blanking [26]. Recently, new methods for in-situ measurements are in development and tested at low punch speeds [8], which enables the determination of strains and strain rates in blanking.

### 1.4. Consequence and approach

This paper aims to determine the energy efficiencies of the tooling and the process that will be used to describe the instability during high-speed blanking. For this purpose, firstly the energy flow during high-speed blanking is analyzed by determining the initial available energy, the corresponding punch speed and its development during the impact. Based on this information, time integration is used to determine the shear work, also incorporating the data from force sensors. Setting the determined energies in relation, the efficiencies of the tool and the process are found. Conclusions about the instability are drawn based on the rate of energy dissipation and homogenized local strains. For the first time, a method is presented to precisely determine the initial kinetic energy and speed, the shear energy required for separation, and the efficiencies between these quantities. The investigated process speed is in a feasible range to generate strain localization and the energy is sufficient to blank parts in one shot.

## 2. Methods

The developed methodologies provide the basis for objective comparisons with existing works on high-speed blanking with different setups.

### 2.1. Setup and measurements

Blanking tests are carried out on an ADIAClip1000J® machine manufactured by MPM France, in which the impact energy is generated by high-speed hydraulics. During the blanking process, a component (called part) is separated from the sheet by shear deformation. A schematic structure of the machine is shown in Fig. 5. An impact bar is accelerated by the release of the pressure of a pressure accumulator (300 bar). The initial machine energy $E_{\text{machine}}$ can be varied continuously between 300 J and 1000 J by adjusting the acceleration length $l_{\text{acc}}$ of the acceleration bar. The geometry of the bar and the mass are constant, so that the impact energy and the speed of the tools cannot be set independently. These energy values are calibrated by the manufacturer (shown in Fig. 5) taking into account internal dissipation and energy losses due to friction. The machine energy is transferred to the tool cassette via a striker bar. This tool cassette contains the punch that transfers the impulse onto the workpiece. The punch can be moved freely for a length $l_{\text{max}}$ until the dampers, and finally, the tool frame absorb the remaining impulse. All experiments are performed with the identical setup, where the diameter of the cylindrical punch was $D_{\text{punch}} = 30$ mm and the total clearance between the die and punch was $c = 0.125$ mm. Tool steel with 61 HRC was used for the punch and die. Three energy settings of $E_{\text{machine}} = 300$ J, 600 J and 900 J were used.

The free body diagrams of the blanked part and the sheet are shown in Fig. 5. The vertical force equilibrium of the system is only valid for punch displacements $l_{\text{punch}}$ smaller than $l_{\text{max}}$. At this displacement $l_{\text{max}}$ (1.6 mm) dampers are reached and energy is dissipated via the dampers in order to reduce the speed of the tool $v_{\text{tool}}$. For all experiments material separation occurred before the dampers got in contact. The dampers are also required for minimizing the oscillation after material separation. Due to the low mass of the ejected part, $m_{\text{part}} \ll m_{\text{tool}}$, the acceleration forces of the part are neglected. In the process, the sheet is clamped in-between the blank holder and the die, and both generate a surface load. Integration of the surface load over the corresponding area results in equivalent forces $F_{\text{tool}}$ and $F_{\text{die}}$. In the process, these forces act on the two sides of the blanking clearance, which causes a torque and a slight bending of the sheet. In this analysis only ideal shear was considered. For simplification it was assumed, that the torques and resulting bending can be neglected, and symmetry for the part can be assumed. In the sheet all forces are projected on a single point, so that the counteracting forces of the torque are considered. The shear force is given by $F_{\text{shear}} = \tau A$, where $\tau$ is the shear stress and $A$ the shear surface of the blanked part. The shear surface $A$ can be estimated by $A = \pi D_{\text{punch}} s$, where $D_{\text{punch}}$ is the diameter of the punch. The measured tool force $F_{\text{tool}}$ includes multiple superposed static forces in the same direction, i.e. the blank holder

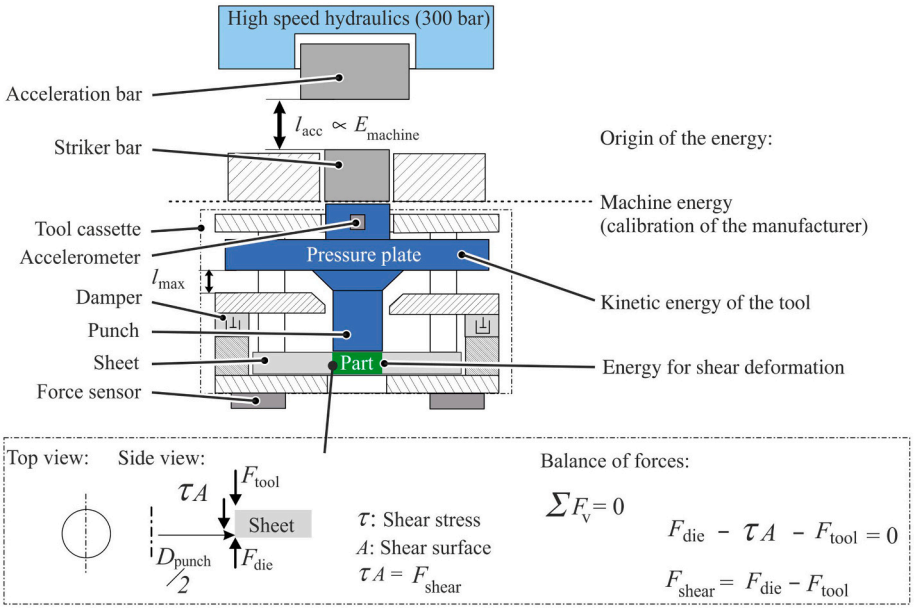


**Fig. 5.** Schematic structure of the tool cassette setup and the corresponding energies and free body diagram of the sheet.

force and the weight of the tool. However, this initial static force $F_{tool}$ is used as an offset value for the measurement and evaluation. This shift is applied before the transmission of the impulse for each experiment. This leads to a direct measurement of the shear forces $F_{shear} = F_{die}$, which are caused by the blanking process.

The positions of the measuring sensors are also shown in Fig. 5. A shock acceleration sensor type PCB Series 350B01 was used, which is capable of measuring up to ±100,000 g. The sensor shows an overall low nonlinearity of ≤2.5 % per 10,000 g. The accelerometer was screwed in the pressure plate, which has a lose connection to the punch during the blanking operation. The measured tool acceleration $a_{tool}$ is used to determine the current speed $v_{tool}(t^*)$ (Eq. 5) and displacement $l_{punch}(t^*)$ (Eq. 6) of the punch at arbitrary time $t^*$ in the process by means of integration over time.

$$v_{tool}(t^*) = \int_0^{t^*} a_{tool}\, dt, \tag{5}$$

and

$$l_{punch}(t^*) = \int_{t_0^*}^{t^*} \int_{t_0^*}^{t^*} a_{tool}\, dt\, dt. \tag{6}$$

The reaction force $F_{die}$ of the tools was determined by four Kistler-Typ 9061A force sensors with a measuring range up to 200 kN. Pocket holes for the sensors are provided on the machine side in the corners underneath the tool. This arrangement would allow to capture an asymmetrical load.

Since the blanking and the occurrence of localization happens in a short duration of time (several µs) the frequency of measurement has to be high. All measurements of the four force sensors and the shock accelerator are synchronized and used with on the same decoder. The maximum sampling rate of 210 kHz was used. A special feature of the process is that the punch is in contact with the sheet prior to the applied impact, leading to a directly transferred load from the striker bar though the punch to the workpiece.

From the punch speed $v_{tool}$, together with the accelerated mass of the punch $m_{tool} = 7.31$ kg, the kinetic energy $E^0_{kin}$ at the impact is determined, assuming rigid body motion ($m_{tool}$ includes the mass of the pressure plate, an attachment for acceleration measurement, and the punch). Using the force sensors, the time of the initialization of the impact $t_0$ and the interval of the force impact $\Delta t = t_1 - t_0$ can be determined (Fig. 6). At this point, $t_0$, a small initial displacement of $l^0_{punch}$ has already occurred as stated. Since the sensors have a background noise, the beginning of the force impact is identified, when a minimum force of 100 N is exceeded. This point in time $t_0$ is used to determine the actual speed $v^0_{tool}$ at the impact, and thus, the initial kinetic energy of the tool $E^0_{kin}$ (Eq. 4) from the acceleration measurements. The impulse is assumed to end at $t_1$ when the force falls below 20 % of the maximum blanking force. The energy for shear deformation $E_{shear}$ (Eq. 3) is then determined via the displacement curve from the acceleration sensors and the force curve during the impulse. It is assumed, that during the impact the ejected part and the tool have the same speed. Therefore, the punch force can be determined by the equivalent shear force $F_p = \tau A$ given in Fig. 5, and ultimately leading to an equivalent formulation as for displacement controlled machines:

$$E_{shear} = \int_{t_0}^{t_1} \tau A \int_{t_0}^{t_1} a_{tool}\, dt dt. \tag{7}$$

In Fig. 6 the method for determining the initial kinetic energy $E^0_{kin}$ at the beginning of the impulse and the determination of the energy for shear deformation $E_{shear}$ are presented. Since the start of the impulse is defined by a minimum force of 100 N, the initial kinetic energy $E^0_{kin}$ is lower than the peak value. The initial kinetic energy $E^0_{kin}$ is identical to the maximum energy available in the process, which can be used for process design. The total dissipated energy $E_{tool}$, measured by the force integration, continues to increase after blanking $t_1$. The rest of the remaining tool kinetic energy, which was not dissipated by shear deformation during the blanking process, is absorbed by the frame and damping elements (Fig. 6b).

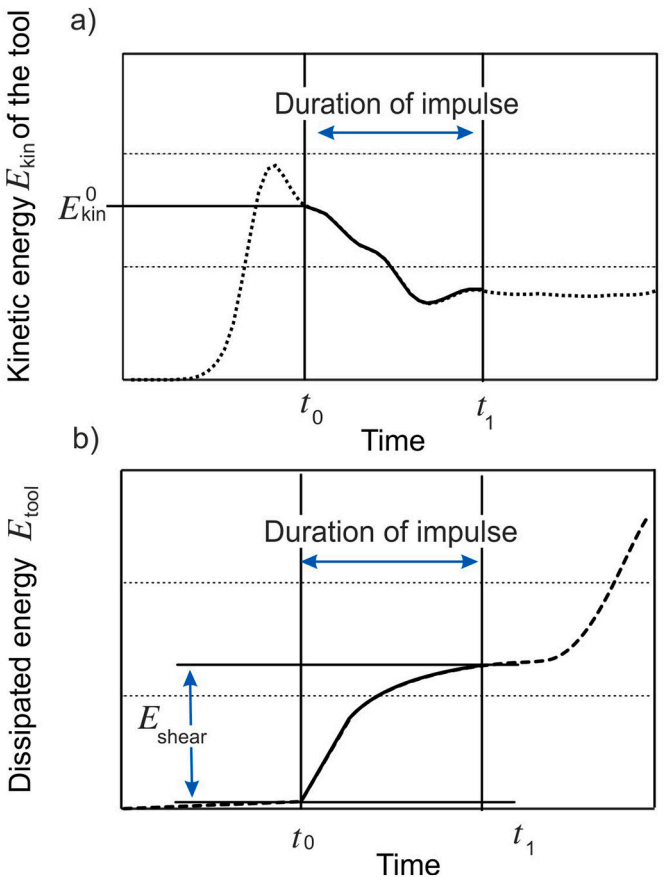


**Fig. 6.** Determination of (a) initial kinetic energy $E^0_{kin}$ and (b) energy for shear deformation $E_{shear}$ during impact as a part of dissipated energy $E_{tool}$.

### 2.2. Efficiencies

For the present machine concept, the energies can be determined separately via the machine energy $E_{machine}$, the kinetic energy $E^0_{kin}$ at the start of the blanking process and the effective energy for the shear deformation $E_{shear}$. Efficiencies can be derived from the corresponding ratios indicated in Fig. 7, where $\eta^{tool}_{machine}$ is the efficiency of the tool. The

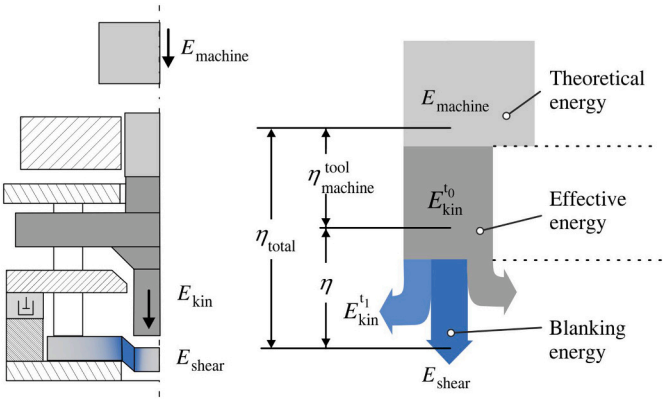


**Fig. 7.** Determination of (a) energies and (b) corresponding efficiencies.

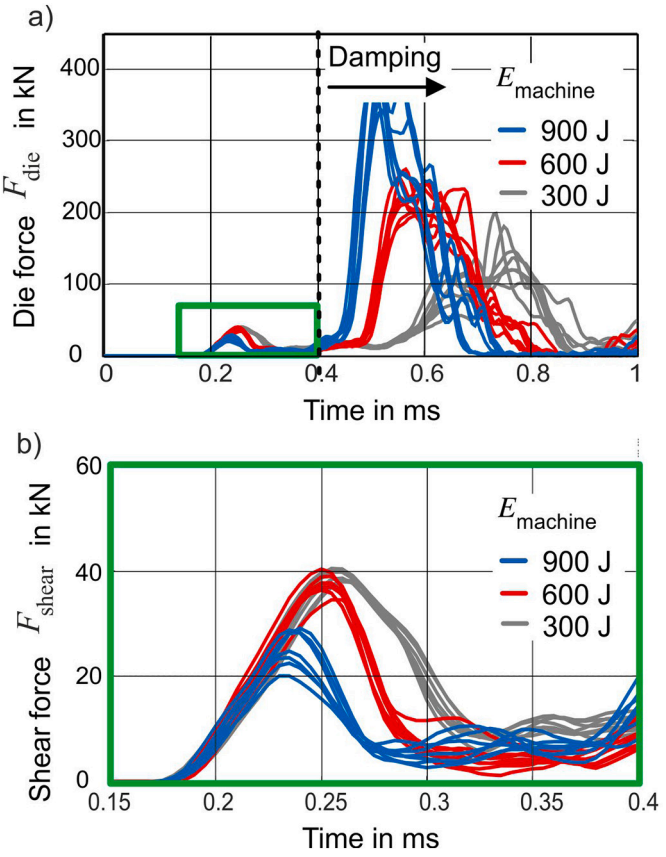


**Fig. 8.** (a) Determination of the measured force $F_{die}$ and (b) the equal shear force $F_{shear}$ for AA5083.

efficiency of the separation $\eta$ (Eq. 8) can be calculated from the measured shear work $E_{shear}$ and the initial kinetic energy $E^0_{kin}$ of the punch.

$$\eta = \frac{E_{shear}}{E^0_{kin}} \tag{8}$$

The highest efficiency $\eta$ would theoretically be achieved when the punch has zero remaining kinetic energy at the time of sheet separation, including no kinetic energy of the ejected part. In general, a high efficiency of the process $\eta$ is preferred. However, the punch speed $v_{tool}$ during the blanking operation decreases, as the efficiency of the process increases. Thus, the local strain rate in the clearance is reduced, the process time is increased, and overall counteracting the aspect of thermal softening in high speed blanking. In this context, total efficiency $\eta_{total}$ can only be used to a limited extent, since it combines the other two efficiencies and does not allow any conclusions to be drawn about the individual components.

### 2.3. Materials

Two different materials, a carbon spring steel C75 and an aluminum alloy AA5083, were investigated. The C75 steel with a thickness of $s_{C75} = 2.1$ mm was analyzed in two states with a reference state of 330 HV10, and in an annealed and hardened state with a hardness of 450 HV10 (C75qt). The hardened C75qt material was used for referencing and will only be discussed with regards to the energy $E_{shear}$. The aluminum alloy AA5083 with a hardness of 85 HV10 and a thickness of $s_{AA} = 1.9$ mm was also investigated. Both materials were blanked with the same tool setup with a diameter of the die of 30 mm and a total clearance of 0.125 mm. Hence, the resulting relative blanking clearance, $c_{rel} = c/s$, for the two materials differs with 6.5 % and 6 % for AA5083 and C75, respectively. For both materials, strips with a width of $b = 39$ mm were used.

## 3. Results and discussions

Using the methods described, the initial speed at the impact and the shear energies for the blanking process are determined. These energies are used to derive the efficiencies of the machine and the process, which can be used for the process design. For the three selected machine energies average initial tool speed of 5.58 m/s, 6.97 m/s and 8.98 m/s are obtained. Material separation was determined by a force drop of 90 %. A corresponding punch displacement between 0.35 mm and 0.95 mm was determined for the different energies and materials. This value increased with increasing initial kinetic energy for the three materials.

### 3.1. Energy requirement and efficiency

The process forces and the displacements of the punch are used to calculate the shear energies.

The evolution of the measured force $F_{die}$ of the die within the first millisecond of the process is shown (Fig. 8a). Afterwards, the system continues to oscillate without another force peak (Fig. 8 and Fig. 9 for AA5083 and C75, respectively). In both figures, two force peaks can be seen, whereby the first force peak is smaller than the second one. The measured process forces are analyzed and compared with those from the conventional blanking process. Estimations for the maximum process forces $F^{max}_{blanking}$ in conventional blanking can be calculated from the ultimate tensile strength $\sigma_{max}$ of the material and the sheared surface $A$ (Eq. 9 from [27]). According to the standard DIN EN ISO 18265 the corresponding ultimate tensile strength $\sigma_{max}$ is 273 MPa for AA5083 and 1088 MPa for the C75 material. This results in maximum process forces $F^{max}_{blanking}$ of 36.7 kN and 170.3 kN for the AA5083 and C75, respectively.

$$F^{max}_{blanking} \approx 0.8\, \sigma_{max}\, A. \tag{9}$$

The first peak of the die force $F_{die}$, here 20–40 N for AA5083 and 120–180 N for C75, is on a similar scale of the estimation of the maximum forces from conventional blanking $F^{max}_{blanking}$. Furthermore, at the time of the force increase ($t_0$), the displacement of the punch is $l^0_{punch} = 0.168$ mm on average and between $l^0_{punch} = 0.05$ mm and 0.28 mm in the extremes. This displacement $l^0_{punch}$ can be related to the gap between pressure plate, punch and attachment of the accelerator, since these parts are not screwed together. Both measures, displacement and force, indicate the first force peak as the force for shearing $F_{shear}$. For both materials the remaining forces $F_{die}$, after the end of the blanking process, are higher in their peak value $F^{max}_{die}$. This second force peak results from the damping of the remaining impulse of the tool. The second force peak is also higher because at this point the remaining momentum must be dissipated within a short distance according to the stiffness of the frame. Consequently, the amplitude of the second peak correlates with the remaining amount of the process energy at the end of blanking.

For the AA5083 aluminum material, for the machine energy $E_{machine}$ of 300 J and 600 J, the maximum shearing force $F_{shear}$ is at a similar level of 38 kN. For the higher machine energy of 900 J, there is a reduction in the maximum process force, which has a relatively high scatter, lying between 19 kN and 26 kN. The reduction of the force $F^{max}_{shear}$ by 30–50 % can be attributed to a possible softening of the material in the form of localization and thermal softening. With the C75 material, the shearing force $F_{shear}$ increases with the increase of the set machine energy $E_{machine}$. For 600 J and 900 J, these are at a similar level of $F^{max}_{shear} = 158$ kN and $F^{max}_{shear} = 172$ kN with a small scatter of 3 kN and 7 kN, respectively. At the lower energy $E_{machine}$ of 300 J, however, the shearing force $F_{shear}$ is reduced to 127 kN and is associated with a significantly wider scatter. The measured force does not drop, but remains at a higher level and rises again. This behavior was observed in all 9 repeated tests. Due to the

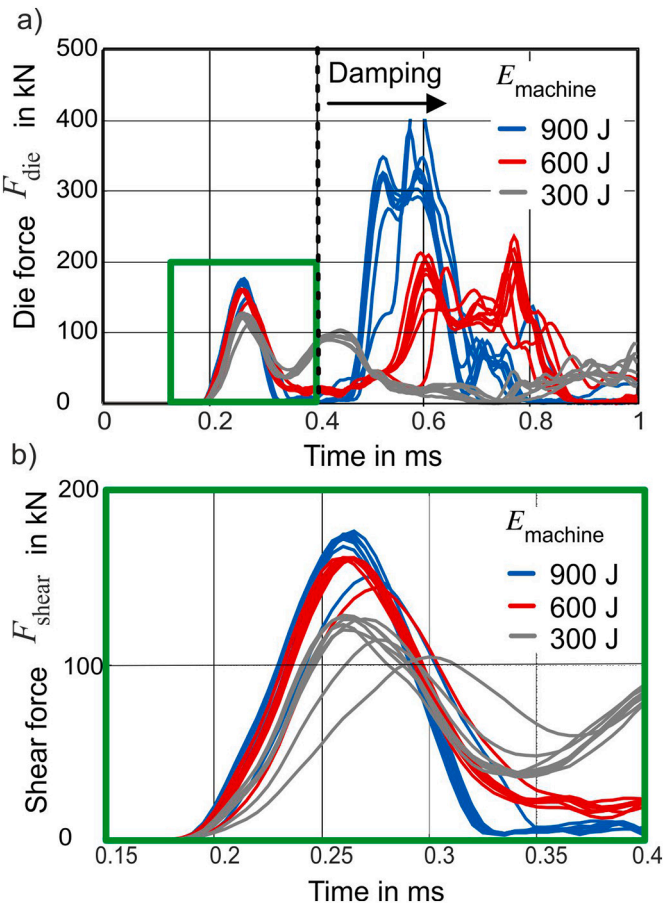


**Fig. 9.** (a) Determination of the measured force $F_{die}$ and (b) the equal shear force $F_{shear}$ for C75.

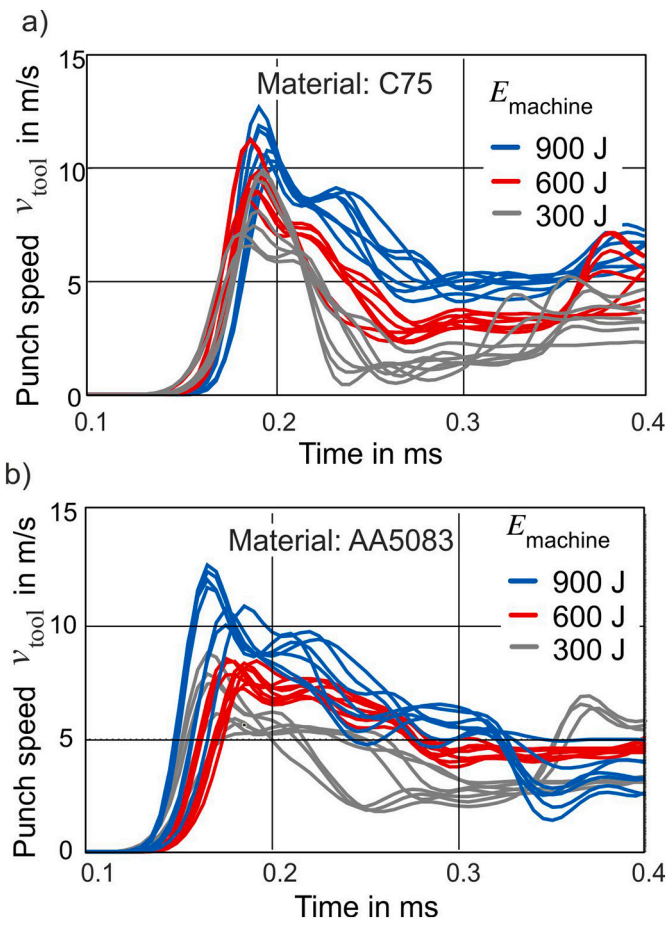


**Fig. 10.** Speed of the punch $v_{tool}$ over time for (a) C75 and (b) AA5083 material.

lower speed of the punch $v_{tool}$ at 300 J, the second force peak caused by the absorption of the remaining momentum would not be present. From this, the conclusion can be drawn that a large part of the impact energy $E^0_{kin}$ was dissipated by the blanking already.

The velocity profiles are given in Fig. 10 for a) C75 and b) AA5083. The highest punch speed occurs after a short acceleration time (< 0.2 ms). The maximum acceleration of the punch determined during blanking for all process parameters was above 26,120 g and reached maximum values of 42,560 g. At the time of the highest speed, no increase in force over the threshold was determined, so that it can be assumed that deformation had not yet taken place, although a punch displacement was determined as stated before. Note that the movement of the sheet part was not measured. Therefore, it cannot be dismissed that elastic waves and vibration are superimposed and can alter the measured force.

From the force-time curves, the duration of the blanking process can be determined. For higher machine energies $E_{machine}$ the average duration of the blanking impulse decreases from 0.13 ms to 0.1 ms, which can be attributed to the higher speed of the punch $v_{tool}$. However, the maximum nominal strain $\varepsilon_{max}$ (Eq. 10) for all materials increases with increasing punch speed $v_{tool}$, meaning that material separation occurs after a larger punch-displacement $l_{punch}$.

$$\varepsilon_{max} = \frac{1}{c}\frac{1}{\sqrt{3}} \int_{t_0}^{t_1} \int_{t_0}^{t_1} a_{tool}\, dtdt. \tag{10}$$

For the lowest machine energy $E_{machine}$, the punch-displacement $l_{punch}$ was in the range of 0.35 mm to 0.52 mm and increased to 0.82 to 1.02 mm at the highest machine energy of 900 J. The corresponding maximum nominal strain $\varepsilon_{max}$ is given in Fig. 11. This combination of

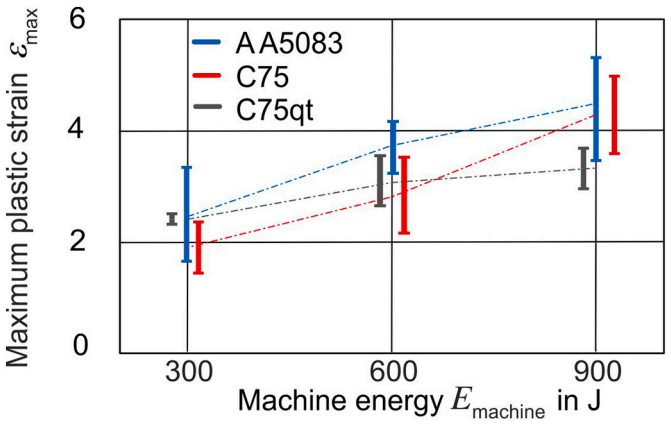


**Fig. 11.** Effect of the machine energy on maximum displacement until material separation.

increasing displacement and reduction of process time leads to a higher temperature in the clearance, due to less time for heat conduction, which ultimately leads to a higher ductility.

For identical values of the machine energy $E_{machine}$ the corresponding kinetic energy $E^0_{kin}$ at the start of the impact $t_0$ was independent of the material investigated. The median for the measured initial kinetic energy $\overline{E}^0_{kin}$ was 114 J, 178 J, and 295 J for a machine energy $E_{machine}$ of 300 J, 600 J and 900 J, respectively. These initial kinetic energies $E^0_{kin}$ are effectively available for the blanking process. The corresponding

average initial tool speed $\bar{v}^0_{tool}$ was 5.58 m/s, 6.97 m/s and 8.98 m/s, respectively. From Fig. 12 the deviation, i.e. total scatter, of the initial kinetic energy $\bar{E}^0_{kin}$ for the three machine energies was determined. The total scatter was 43 J, 95 J and 94.5 J with a corresponding scatter of initial tool speed $v^0_{tool}$ of 1.02 m/s, 1.77 m/s and 1.31 m/s for a machine energy $E_{machine}$ of 300 J, 600 J and 900 J, respectively. The energy difference between $E_{machine}$ and $E^0_{kin}$ is lost through the transfer of momentum and in kinetic energy of the impact bar through acceleration in the opposite direction. This loss in energy cannot be used directly for the process, however, it can interfere at later stages with the punch, if re-strikes occur between the punch and striker bar. The initial kinetic energy $E^0_{kin}$ relates linearly to the adjusted machine energy $E_{machine}$ (Fig. 12). Although a trend of increasing kinetic energy with machine energy can be determined, for this setup an analysis of the machine energy in a strict sense can be misleading. For a constant machine energy, the scatter leads to a partial overlapping of kinetic energy, i.e. single experiments with a set machine energy of 600 J may result in a kinetic energy higher than a single experiments at 900 J (see e.g. 267 J vs 243 J for a lower and higher machine energy, respectively). The efficiency $\eta^{tool}_{machine}$ (Eq. 11) of the impact transmitted by the tool can be determined as the slope of the gray band in Fig. 12a). As can be seen from Fig. 12b) the efficiency of the tool decreases slightly with increasing machine energy.

$$\eta^{tool}_{machine} = \frac{E^0_{kin}}{E_{machine}} \approx 0.28 \tag{11}$$

By evaluation of the data from [21], where a similar hydraulic system but different tool setup was used, efficiencies $\eta^{tool}_{machine}$ between 26.96 % and 103 % are achieved. With increasing machine energy $E_{machine}$, a decrease in efficiency $\eta^{tool}_{machine}$ could also be determined. However, the authors do not provide the spread of the velocity data. Determining the kinetic energy $E^0_{kin}$ from the given mass ($m_{tool}$= 9.95 kg) and the speed of the punch ($v_{tool}$= 7.2 m/s) and putting it in relation to the machine energy $E_{machine}$, this would correspond to the unrealistic efficiency $\eta^{tool}_{machine}$ of 103 %. In order to draw a conclusion for the resulting properties of the sheared surface and dissipated energy by shear deformation, the specific tool speed of a single experiment should be considered.

The energy for shearing $E_{shear}$ during the impulse is determined for the two workpiece materials and the three machine energies $E_{machine}$ (Fig. 13). In Fig. 13 the specific energy $\bar{E}_{shear}$ required for blanking is shown, by normalizing the shear energy by the shear area $\bar{E}_{shear} = E_{shear}/A$. The appearance of both figures a) and b) is similar, but reflects the difference in sheet thickness of the materials. As can be anticipated from the shear force $F_{shear}$ curves, the energy for shear deformation is significantly lower for the aluminum AA5083 material than for the carbon steels C75 and its hardened version C75qt. The required shear

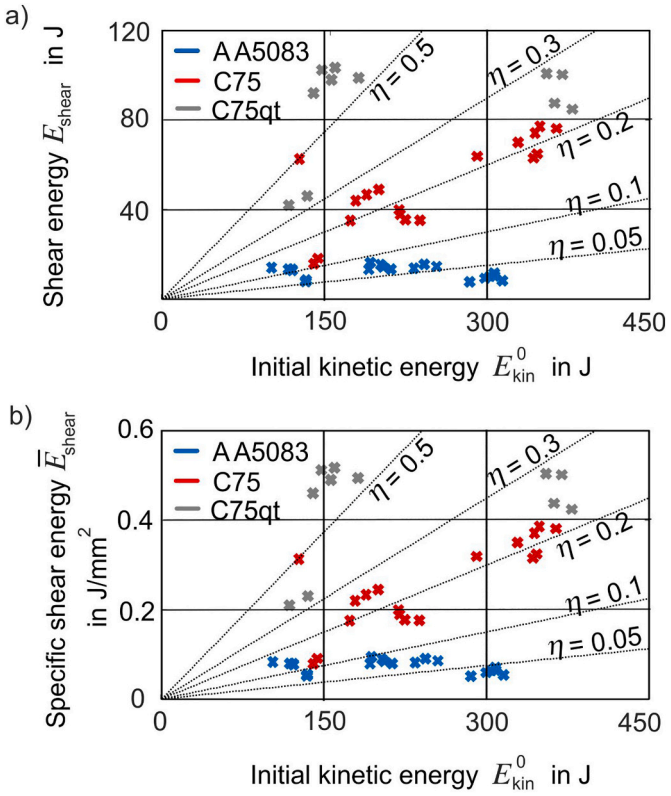


**Fig. 13.** (a) Total $E_{shear}$ and (b) specific $\bar{E}_{shear}$ dissipated energy by shearing until material separation of the resulting kinetic impact energies $E^0_{kin}$ and materials. Lines of constant efficiencies $\eta$ have been added for classification.

energy $E_{shear}$ for AA5083 material was between 7.3 and 13.9 J, 13.8–16.0 J and 8.8–12.8 J for initial kinetic energies of $E^0_{kin} \approx 120$ J, 240 J and 300 J, respectively. Despite the large relative scatter of almost 50 % in shear energy $E_{shear}$ for low machine energies, the total scatter is almost constant. With the increase of the machine energy the initial punch speed increases, however no direct influence of the punch speed $v_{tool}$ on the necessary shear energy $E_{shear}$ can be found for the AA5083 material. For the material C75, a clear tendency in the relation between the initial kinetic energy $E^0_{kin}$ and the shear energy $E_{shear}$ can be seen. From this it can be derived that the flow stress of the material increases significantly at higher strain rates [28] (despite the probably also higher thermal softening), and thus is more sensitive to changes in strain rates. This leads to shear energies on average of $E_{shear}$ = 16.3 J at $E^0_{kin} \approx$150 J, while at $E^0_{kin} \approx$ 380 J the shear energy $E_{shear}$ = 71.1 J is more than four

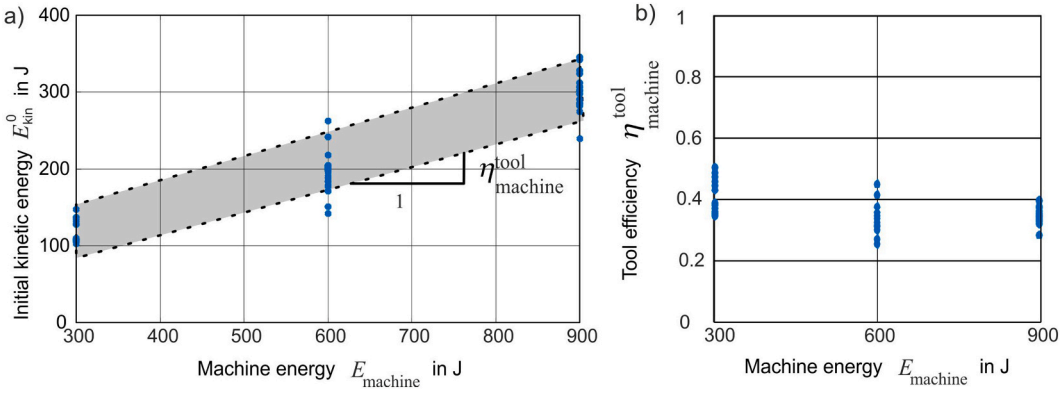


**Fig. 12.** a) Correlation between set machine energy $E_{machine}$ and resulting initial kinetic energy $E^0_{kin}$ of the punch. The efficiency $\eta^{tool}_{machine}$ is given by a) the derivative and b) for each data point.

times higher.

The increase of the energy $E_{shear}$ between the lowest and highest initial kinetic energy $E^0_{kin}$ by a factor of 4 may be due to a high strain rate sensitivity of the material. Due to the increased punch speed, the strain rate $\dot{\varepsilon}$ increases linearly (Eq. 1) and thus increases the energy required to maintain the deformation at the rate specified by the speed of the punch $v^0_{tool}$.

As stated in the Section 2, the used energy for deformation $E_{shear}$ of the AA5083 is lower, also the efficiency of the separation $\eta$ for the aluminum material is lower compared to the C75 material. For the design of the process, the energy $E^0_{kin}$ could be reduced, since at the end of the process a large part of the energy is dissipated by the dampers. The characteristic of the process depends on the strain rate in the blanking clearance $c$. In order to achieve a higher efficiency at the same strain rate the mass of the punch has to be reduced. Alternatively, multiple parts could be blanked with the same setup to increase the efficiency $\eta$.

### 3.2. Characteristics of the blanked surface

Since one of the objectives of high-speed blanking is to create sheared edges of high quality, the geometrical edge properties and the corresponding light microscope images are evaluated. An overview of the values is given in Table 2.

Although Fig. 12 shows that the machine energy $E_{machine}$ is not an objective description, it is used for general classification. The kinetic energies can have a partial overlap due to the scattering. Therefore, these classifications should not be interpreted sharply. For the evaluation in this section, single experiments with speeds in the range of the specified mean value were used. The blanked surface of the aluminum AA5083 for the three energies $E_{machine}$ is investigated with the objective of a qualitative comparison of the sheared edges (Fig. 14). The section cuts are evaluated in terms of rollover and mean straightness. For all machine energies the sheared edges show a low rollover (≈5–6 %) and low deviation in straightness (≈2.7 %) of the blanked surface. However, a small burr was found for the lowest and largest machine energy $E_{machine}$ with a length of 12 µm and 16 µm. Two crack fronts met in the middle (a) at the lowest machine energy $E_{machine} = 300$ J and caused a difference in the straightness of the surface of 50 µm. The shear-affected zone $w$ can be determined from optical images of microstructure, where transformed shear bands are white, due to the grain size in the range of nanometer, where in deformed shear bands the grains are tilted. The aluminum with the medium energy ($E_{machine} = 600$ J) shows the lowest width of 15 µm, while the width for 300 J and 900 J are 41 and 37 µm, respectively (determined from Fig. 14 with polarizing filter, which is not visible here). For each analyzed specimen the machine energy $E_{machine}$, the kinetic energy, and the impact speed are given in the figure denoted by $E^0_{kin}$ and $v_0$, respectively. At $E_{machine} = 600$ J the energy dissipation by the material $E_{shear}$ is higher, which could indicate a onset of localized deformation throughout the thickness of the sheet, resulting in a higher surface quality in contrast to $E_{machine} = 300$ J. As a result of thermal softening at higher punch speeds the energy decreases further, while keeping a high surface quality.

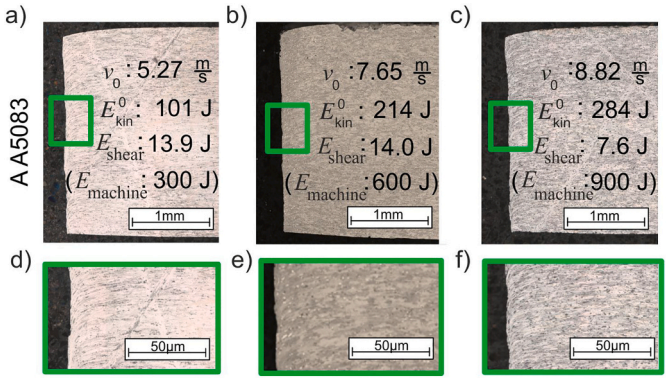


**Fig. 14.** Sheared edge of AA5083 material for machine energies $E_{machine}$ of 300 J (a), 600 J (b) and 900 J (c) and the corresponding kinetic energies $E^0_{kin}$ and tool speed $v_0$. The effect on the resulting sheared edge is given in d), e), and f), respectively.

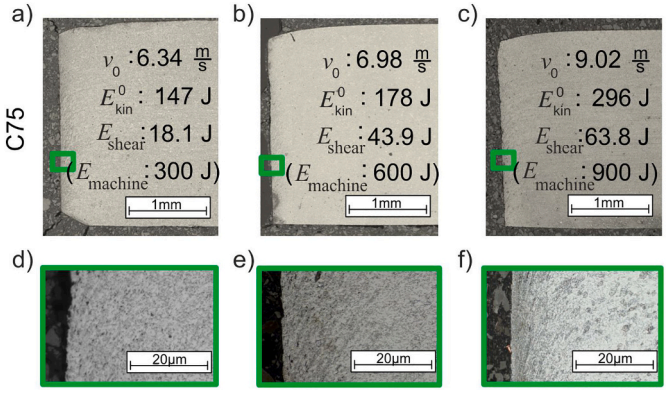


**Fig. 15.** Sheared edge of C75 material for machine energies $E_{machine}$ of 300 J (a), 600 J (b) and 900 J (c) and the corresponding kinetic energies $E^0_{kin}$ and tool speed $v_0$. The effect on the resulting sheared edge is given in d), e), and f), respectively.

The sheared edge for the carbon spring steel C75 show similar results in straightness (Fig. 15). For all three energies the rollover was in the range of 112–143 µm. The straightness was determined by the maximum deviation in radial direction of the sheared surface, which was between 49 µm - 92 µm. Despite the increase of energy dissipation $E_{shear}$ with tool speed $v_0$, the size of the shear affected zone (39–43 µm) is almost constant. Since only the tool speed is changed, which affects the homogenized strain rate $\dot{\bar{\varepsilon}}_{eff}$, the strain rate sensitivity of the material can cause the only increase in flow stress $\tau$. While the strain rate sensitivity for C75 material is relatively large $m^{C75} = 0.0104$ [10], AA5083 shows no or in some strain rate regimes negative strain rate sensitivity $m^{AA5083} \approx 0$ [28].

For the hardened C75qt material (Fig. 16) the lowest machine energy

**Table 2**
Table of surface properties blanked [29] with various machine energies.

| Material | Machine energy | Kinetic energy | Rollover | Straightness | Burr size |
|---|---|---|---|---|---|
| AA5083 | 300 J | 101 J | 115 µm (6.1 %) | 50 µm (2.6 %) | 12 µm |
| | 600 J | 214 J | 109 µm (5.7 %) | 46 µm (2.4 %) | < 5 µm |
| | 900 J | 284 J | 126 µm (6.6 %) | 58 µm (3.1 %) | 16 µm |
| C75 | 300 J | 147 J | 143 µm (6.8 %) | 49 µm (2.3 %) | < 5 µm |
| | 600 J | 178 J | 130 µm (6.2 %) | 75 µm (3.5 %) | < 5 µm |
| | 900 J | 296 J | 112 µm (5.3 %) | 92 µm (4.3 %) | < 5 µm |
| C75qt | 300 J | 143 J | 73 µm (3.5 %) | 46 µm (2.2 %) | < 5 µm |
| | 600 J | 188 J | 74 µm (3.5 %) | 109 µm (5.2 %) | < 5 µm |
| | 900 J | 378 J | 76 µm (3.6 %) | 52 µm (2.4 %) | < 5 µm |

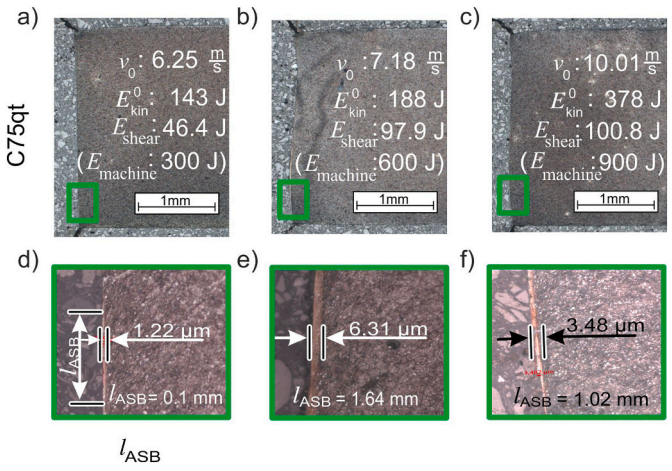


**Fig. 16.** Sheared edge of C75qt material for machine energies $E_{machine}$ of 300 J (a), 600 J (b) and 900 J (c) and the effect on the resulting microstructure (d), (e) and (f), respectively.

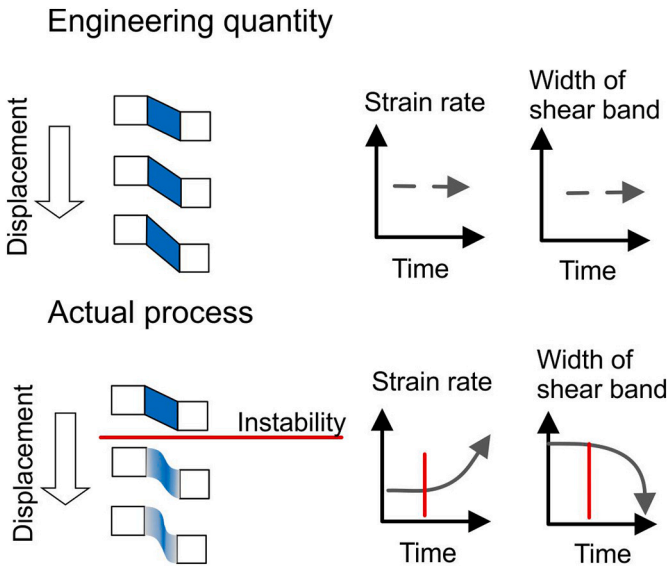


**Fig. 17.** Comparison of engineering and true local quantities of deformation referring to shear band width and strain rate distribution (blue sketch) and evolution (graphs) for a constant tool speed. (For interpretation of the references to color in this figure, the reader is referred to the web version of this article.)

$E_{machine}$ of 300 J shows the highest straightness, while for $E_{machine}$ 600 J and 900 J an S-shape can be seen. The lower the straightness, the higher the resulting width of the transformed shear band, $l_{ASB}$. For the lowest machine energy $E_{machine}$ (300 J), a very short (36 µm) and thin (1.22 µm) ASB can be seen in the lower region. This thickness becomes larger at 900 J (3.48 µm) and has the highest width at 600 J of 6.31 µm. At a medium machine energy $E_{machine}$ the deflection of the S-shape is the highest. These results are in good agreement with the investigations of a high strength steel material by Winter et al. [21], despite only kinetic energy was used. The highest straightness was reported [21] for low machine energies, while the length and thickness of the ASB decreases from 730 µm to 310 µm and 7 µm to 1 µm, respectively.

Consequently, the initiation of a shear band and the actually sheared volume has a direct influence on the blanked surface. The same behavior can be seen in the amount of dissipated energy by the material. The shear energy $E_{shear}$ increases by a factor of 2 between machine energies $E_{machine}$ of 300 J and 600 J. For machine energies $E_{machine}$ of 600 J and 900 J, the shear energy $E_{shear}$ is at a similar level ( $E_{shear}$ = 70–100 J), while the width of the transformed shear band decreases at higher tool speeds $v_0$. This concentrates the energy $E_{shear}$ in a smaller area and results in a higher shear deformation in the transformed shear band. The energy analysis shows that, if a transformed adiabatic shear band (ASB) occurs (white layer), the required energy for blanking is higher in comparison to blanking at lower tool speed without formation of such a band. This is initially surprising, since the strain localization is expected to reduce the flow stress by thermal softening. However, the achieved strains are higher, since the formation of transformation shear bands allows a higher strain in a smaller volume to be absorbed before failure and with that the shear energy $E_{shear}$ increases.

### 3.3. Localization analysis

For the formation of adiabatic shear bands, a high strain localization is necessary; the point in time at which this localization occurs can be estimated using the instability analysis. In Recht's [2] criterion, the instability is reached when the shear stress no longer increases with increasing deformation ($d\tau \backslash d\varepsilon < 0$). For blanking, such a shear stress $\tau$ can be calculated via the process force $F_{shear}$ and the sheared area $A$. In the following, engineering strains $\varepsilon$ can be determined by the known clearance $c$ and punch displacement $l_{punch}$ (see time integration of Eq. 6). Accordingly, the instability criterion for blanking reads:

$$\frac{d\tau}{d\varepsilon} = \frac{d(F_{shear}/A)}{d(l_{punch}/c)1/\sqrt{3}} \leq 0. \tag{12}$$

A homogeneous deformation until the onset of localization can be assumed, such that the engineering shear stress $\bar{\tau} = F_{shear}/A$ can be determined by the measured force $F_{shear}$ and the sheared area $A$ shear, directly. For a homogeneous shear deformation within the blanking clearance $c$, the plastic strains $\varepsilon$ can be determined via the displacement $l_{punch}$ of the punch by integration over time of Eq. 6). The strains in the blanking clearance $c$ = 0.125 mm are not constant but change in radial direction. Since the size of the clearance is small in relation to the tool diameter $D_{punch}$, the error in strain for the used setup can be determined by $\varepsilon_{error} = D_{punch}/(D_{punch} + 2c) < 1\%$. In the high-speed blanking process the shear-affected zone can be smaller due to shear localization (Fig. 2) and results in a different strain distribution. For the energy analysis in the following it is assumed that the deformation occurs in a homogeneous manner in the corresponding volume in the clearance and no shearing-off occurs during the process. This assumption leads to engineering quantities instead of true values (Fig. 17). This engineering approach helps for a qualitative comparison of different effects of tool speeds on material properties, since localization effects (Fig. 2) can vary with the material and the process speed. For the analysis of local effects, this approach underestimates the local energy dissipation and thermal softening effect. In addition, geometrical and material-based instabilities cannot be separated.

The total energy up to complete separation was determined in the previous section. The strains in high-speed blanking can be localized within the clearance and lead to a softening of the material, which is reflected in the shear energy curve. By the dissipated shear energy the required amount of energy until localization, and the energy dissipation between localization and material separation is determined. In order to find the point in time of separation, and the onset of localization, the instability criterion of Recht applied to the blanking kinematic was evaluated (Eq. 12). With the measured quantities, the derivative of the engineering shear stress $\nabla_\varepsilon \bar{\tau}$ is equivalent to the instability formulation by Recht [2]. The point of the onset of localization can be evaluated, when the engineering shear stress $\bar{\tau}$ reaches a maximum value, meaning

$$\nabla_\varepsilon \bar{\tau} = 0. \tag{13}$$

As an alternative, the dissipated energy can also be used as a measure for the instability criterion directly, since both approaches can be

transferred assuming a homogeneous deformation. Since the shear energy is expressed by $E_{shear} = \int \tau\, A\, dl$ and the strains can be transformed by $d\varepsilon = dl/(c\sqrt{3})$ the energy-based instability criterion reads $\nabla E = dE_{shear}/d\varepsilon$ and can be interpreted as a flow stress $\sigma_y$ over the volume $V$ in the clearance. This is not unique for blanking and can also be found by the general form of energy relation $dE_{shear} = V\,\sigma_y\,d\varepsilon$ and enables the instability analysis regardless of the way of energy determination. In addition, the energy for shear deformation $E_{shear}$ increases monotonically during the impulse, so by the derivative $\nabla E_{shear} = dE_{shear}/d\varepsilon$ the pivot point of hardening and local softening can be captured directly.

The distribution of the engineering shear stress $\bar{\tau}$ over the strains $\varepsilon$ is shown in Fig. 18, were the individual curves are omitted for a better overview and only the envelope curves are shown. The maximum strain $\varepsilon_{max}$ (Eq. 10) for all materials increases with increasing machine energy $E_{machine}$, and punch speed $v_{tool}$, accordingly. For the aluminum material strain values of $\varepsilon_{max} \approx 4$ and for C75 between $3.5 \leq \varepsilon_{max} \leq 3.9$ were reached.

The derivative of shear stress $\nabla\bar{\tau}$ (Eq. 12) of the C75 and C75qt material where significantly higher by a factor of 6 than for the aluminum material, which results in a higher energy dissipation for the same deformation. In light of the conversion of plastic power into heat, in terms of β is the Taylor-Quinney coefficient [30], the flow stress $\sigma$, the density $\rho$, the heat capacity $c_p$ and the rate of temperature $\dot{T}$

$$\beta\,\sigma\dot{\varepsilon} = \dot{T}\rho c_p. \tag{14}$$

$\nabla\bar{\tau}$ also gives a measure of the thermal energy generated. From the force curves it could already be seen that there was no direct drop like in conventional blanking, but rather slowly decreases. After reaching the maximum engineering shear stress $\bar{\tau}_{max}$, about 60 % of the equivalent strain $\varepsilon$ is reached and the strength of the material decreases.

Comparing the two C75 materials, $\nabla\bar{\tau}$ for the C75qt material is larger for medium and high machine energies (600 J and 900 J). After reaching the point of instability (Eq. 13) $\nabla\bar{\tau}$ is also higher, indicating a higher strain localization or softening of the material. Besides a larger $\nabla\bar{\tau}$-value for a higher tool speed $v_{tool}$, the time period of the impulse is also shorter. This results in a higher induced thermal energy rate and lower heat conduction. Both observations accelerate the effect of thermal softening in the material, leading to a smaller shear affected zone $w$ as shown in Fig. 16 e) and f). On a macroscopic level the separation of the C75qt material at a machine energy of 900 J is reached after a larger punch displacement, indicating a higher ductility $\varepsilon_{max}$. But the local strain distribution across the thickness of the sheet is varying, as can be seen by the area with and without shear bands (Fig. 16). Therefore, it is not possible to determine the effective local strains, but qualitatively the shear-affected zone $w$ is smaller than the blanking clearance $c$ (like Fig. 2). However, this information is not available a priori, so the blanking clearance suits as a first approximation. It can be concluded, that the energy introduced into the shear-affected volume is underestimated and the effective derivative of shear stress keeps, on a local level, further increasing rather than decreasing. This would favor a further increase of specific thermal energy and an increase in strain localization. The exact interaction of the strain localization and the point in time when the localization occurs cannot be determined on the basis

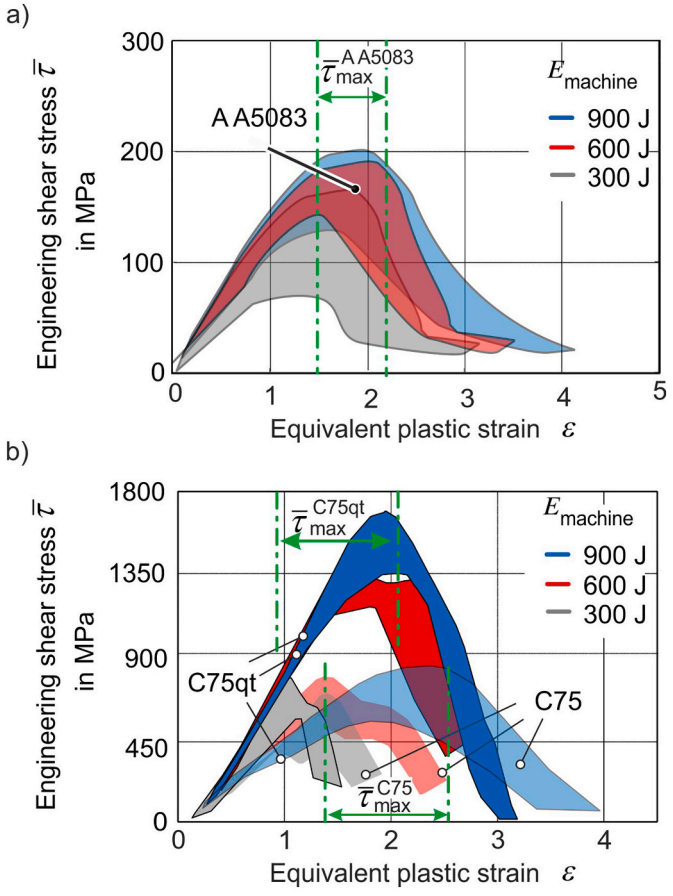


**Fig. 18.** The engineering shear stress $\bar{\tau}$ with respect to the plastic strain $\varepsilon$ for (a) aluminum, (b) C75 and C75qt material. The peak shear stress $\bar{\tau}_{max}$ denotes the point of instability. It is important, that engineering quantities (Fig. 2) were used and homogeneous pure shear deformation in the clearance is assumed (Eq. 5).

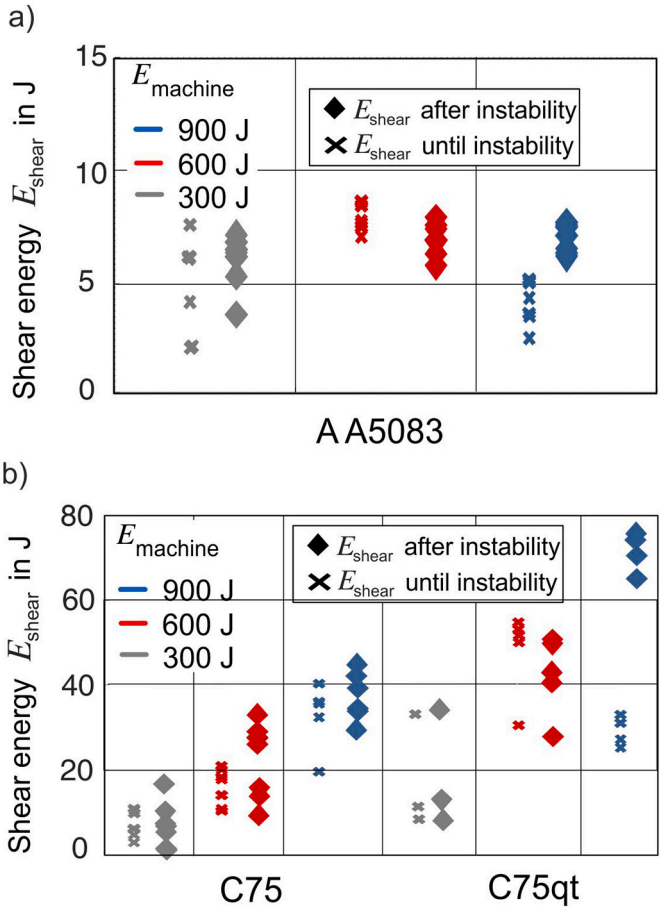


**Fig. 19.** Energy required for deformation $E_{shear}$ until the instability (cross) and between instability and material separation (diamond) for (a) aluminum, (b) C75 and C75qt material.

**Table 3**
Table of the three approximation to describe local energy dissipation normalized by volume.

| | Machine energy | Kinetic energy | $\widehat{E}$ in $J/mm^2$ | $\widetilde{E}_c$ in $J/mm^3$ | $\widetilde{E}_{mix}$ in $J/mm^3$ | $\widetilde{E}_w$ in $J/mm^3$ |
|---|---|---|---|---|---|---|
| AA5083 | 300 J | 101 J | 0.07 | 1.1 | 2.3 | 3.4 |
| | 600 J | 214 J | 0.07 | 1.9 | 3.6 | 7.5 |
| | 900 J | 284 J | 0.04 | 1.2 | 2.5 | 4.1 |
| C75 | 300 J | 147 J | 0.09 | 1.8 | 3.9 | 5.8 |
| | 600 J | 178 J | 0.22 | 1.7 | 4.0 | 5.3 |
| | 900 J | 296 J | 0.32 | 5.8 | 14.2 | 17.0 |
| C75qt | 300 J | 143 J | 0.23 | 5.8 | 373.2 | 596.4 |
| | 600 J | 188 J | 0.49 | 5.5 | 51.6 | 108.6 |
| | 900 J | 378 J | 0.51 | 9.2 | 225.5 | 335.7 |

of the measured curves and remains unknown.

The instability criterion (Eq. 13) can be used to separate the amount of energy dissipated in the material $E_{shear}$ until the instability $E^{x}_{shear}$ (i.e. the area under the force-displacement curve until the maximum) and after $E^{\diamond}_{shear}$ (i.e. the area under the force-displacement curve from the maximum on). This split provides an insight of how much energy is necessary to cause the instability $E^{x}_{shear}$ (cross in Fig. 19) and, on the other hand, the amount of energy the material can dissipate from the instability until material separation $E^{\diamond}_{shear}$ (diamond in Fig. 19). For the machine energy of 300 and 600 J, the energy levels of the two split energies are on a comparable level (excluding aluminum at 300 J, where two cracks occurred from opposite sites). With increasing machine energy $E_{machine}$, the amount of energy dissipated until the point of instability (diamond) is increased. Additionally, with increasing tool speed, the amount of energy required from the point of instability until material separation increases as well. Furthermore, for the machine energy of 900 J, the ratio of the energy dissipation until the instability and afterwards $R_{shear} = E^{\diamond}_{shear}/E^{x}_{shear}$ is significantly larger, $R^{AA}_{shear}$ =1.6 (aluminum), and $R^{C75qt}_{shear} = 2.4$ (C75qt) in comparison to the other investigated energies ($R^{*}_{shear} \approx 1 \pm 0.2$). In particular, for the C75qt material this indicates, that to maintain the strain localization with a thin high-energy adiabatic shear band (ASB) formation, a significant amount of energy is required.

With his analysis three different approximation of the dissipated energy per volume can be established. While the thickness and the radial position of the sheared volume is fixed, the sheared volume can be estimated by the open parameter of the clearance $c$, the shear-affected zone $w$ or a mixture of both. While for the first two approaches the shear energy $E_{shear}$ is divided by the respective volume, leading to an lower bound $\widetilde{E}_c$ and an upper bound $\widetilde{E}_w$, the mixed method uses both. By normalizing the energy until the instability $E^{x}_{shear}$ to the volume in the clearance $c$, and the amount after instability $E^{\diamond}_{shear}$ to the volume corresponding to the shear-affected zone $w$. The respective energy per volume is denoted as and $\widetilde{E}_{mix}$ and suits as an optimized enhanced estimation. This analysis can be used to estimate the temperature or volume based energy dissipation for establishing of ASB in high-speed blanking. Table 3 presents a comparison of the various approaches. The shear energy per blanked surface $\widehat{E} = E_{shear}/A$ on the other hand can be used as a technological parameter for process design and is included for reference.

Ultimately, for AA5083 and C75 the difference between the lower and upper limit is separated by a factor of 4 and the refined normalized energy is in-between the upper and lower limit, whereby this tends towards the upper limit. In contrast, for C75qt material the upper and lower limit is separated by a factor of 20 up to 100. This indicates that the localized deformation causes the dissipation of excessive local energy. Furthermore, there is a strong agreement between the upper bound approach and the improved energy computation.

## 4. Conclusion

A new tool concept was used to determine the dissipated energy during high-speed blanking, while the initial kinetic energy was also determined. For the first time blanking forces, shear energy, and initial kinetic energy were investigated simultaneously, allowing the assessment of actual efficiencies. For the three investigated materials the amount of dissipated shear energy $E_{shear}$ was determined for various initial kinetic energies. Based on this, the following conclusions can be drawn:

1) The use of the machine energy $E_{machine}$ is inappropriate to derive the effective available kinetic forming energy $E^{0}_{kin}$, since it is dependent on the efficiency of the tool.
2) While high total efficiencies are generally favored, is should be noted that this leads to a reduction in tool speed. This increases the amount of conducted heat and may negate the effect of thermal softening. However, a high remaining energy makes the process more reliable, but the energy has to be dissipated by the tool frame after material separation and it increases the impact load of the punch, which is not desirable for its lifetime.
3) The energy split of the shear energy $E_{shear}$ by the instability criterion reveals - across all investigated materials – that more energy is dissipated after the instability. In addition, the materials show an increasing maximum nominal strain $\varepsilon_{max}$ prior separation, with the increase of punch speed $v_{tool}$. This could be attributed to temperature and localization effects of the material. The energy required $E_{shear}$ increases by a factor of 2–2.5 for the case of a formation of an adiabatic shear band in comparison to no shear band formation.

   However, the findings on the formability $\varepsilon_{max}$ are based on the strict assumption of a homogeneous distribution of strains in the clearance. A validation or falsification by in-situ methods of strain determination, e.g. as described in [31], could improve the knowledge and would connect the energy dissipation with the local distribution.
4) An estimated normalized energy dissipation was determined using the volumes affected by shear and the experimentally obtained shear energies. When the sheet thickness varies, this value can be utilized to calculate real energy requirements. Furthermore, it can be utilized to estimate local temperature development in the shear zone.
5) The energy required for shear deformation $E_{shear}$ for blanking of aluminum was not dependent on the punch speed (impact speeds of $v^{0}_{tool} = 5.2$–$10.9$ m/s investigated), which is not the case for C75. This is in agreement with a higher strain rate sensitivity of the steel materials (ref. [10,28]).
6) The surface quality among all investigated parts shows only small deviations in rollover, burr size, and straightness with respect to the initial kinetic energy.
7) At least with this tool setup, a severe variation of initial tool speed for an identical machine setup was investigated, such that for specific samples there are overlaps. In review, these variations can also be found in other papers but are not explicitly stated. For a proper

comparison in high speed blanking, it seems useful to determine process quantities, like energies, for each individual process.

## CRediT authorship contribution statement

**Fabian Schmitz:** Conceptualization, Data curation, Formal analysis, Investigation, Methodology, Validation, Visualization, Writing – original draft, Writing – review & editing. **Till Clausmeyer:** Formal analysis, Funding acquisition, Project administration, Supervision, Writing – review & editing, Conceptualization. **Marlon Hahn:** Conceptualization, Formal analysis, Investigation, Supervision, Writing – review & editing. **A. Erman Tekkaya:** Funding acquisition, Project administration, Resources, Supervision, Writing – review & editing, Conceptualization.

## Declaration of competing interest

The authors declare that they have no known competing financial interests or personal relationships that could have appeared to influence the work reported in this paper.

## Acknowledgements

The authors wish to thank the German Research Foundation (DFG) for their funding and support during the project “Application and analysis of adiabatic blanking” (Project number 428780322). In addition, we like to thank the LWW in Chemnitz for the heat treatment of the C75 material.

## References

[1] Davies R, Dhawan SM. A preliminary investigation of high-speed blanking and piercing of metals. Proc Inst Mech Eng Conf Proc 1965;180:182–96. https://doi.org/10.1243/pime_conf_1965_180_243_02.
[2] Recht RF. Catastrophic thermoplastic shear. J Appl Mech Trans ASME 1964;31:189–93. https://doi.org/10.1115/1.3629585.
[3] Dodd B, Bai Y. Adiabatic shear localization. Elsevier Ltd; 2012.
[4] Johnson W, Slater RAC. Further experiments in quasi-static and dynamic blanking of circular discs from various materials. Proc Inst Mech Eng Conf Proc 1965;180:163–81. https://doi.org/10.1243/pime_conf_1965_180_242_02.
[5] Mikkers JC. High speed blanking. Ann CIRP 1969;17:269–78.
[6] Davies R, Dhawan SM. Comparison of some strain rate effects in slow and high speed blanking. In: Proc 9th Int Mach Tool Des Res Conf; 1968. p. 135–48.
[7] Balendra R, Travis FW. Static and dynamic blanking of steel of varying hardness. Int J Mach Tool Des Res 1970;10:249–71. https://doi.org/10.1016/0020-7357(70)90010-7.
[8] Johnson W, Travis FW. High-speed blanking of steel. Eng Plast 1968:380–400.
[9] Tekiner Z, Nalbant M, Gürün H. An experimental study for the effect of different clearances on burr, smooth-sheared and blanking force on aluminium sheet metal. Mater Des 2006;27:1134–8. https://doi.org/10.1016/j.matdes.2005.03.013.
[10] Schmitz F, Winter S, Clausmeyer T, Wagner MFX, Tekkaya AE. Adiabatic blanking of advanced high-strength steels. CIRP Ann 2020;69:269–72. https://doi.org/10.1016/j.cirp.2020.03.007.
[11] Zener C, Hollomon JH. Effect of strain rate upon plastic flow of steel. J Appl Phys 1944;15:22–32. https://doi.org/10.1063/1.1707363.
[12] Gutknecht F, Steinbach F, Hammer T, Clausmeyer T, Volk W, Tekkaya AE. Analysis of shear cutting of dual phase steel by application of an advanced damage model. Procedia Struct Integr 2016;2:1700–7. https://doi.org/10.1016/j.prostr.2016.06.215.
[13] Landgrebe D, Barthel T, Schieck F. Trimming of flat and tubular components by high speed impact cutting. In: Proc. ASME 2017 Int. Mech. Eng. Congr. Expo. Springer; 2018.
[14] Gaudilliere C, Ranc N, Larue A, Maillard A, Lorong P, Gaudilliere CUA. High speed blanking : an experimental method to measure induced cutting forces. Exp Mech Soc Exp Mech 2014;53(7):1117–26.
[15] Davies R, Dhawan SM. Further developments in high-speed blanking of metals. In: Proc. 7th Int. Mach. Tool Des. Res. Conf.; 1966.
[16] Johnson W, Slater RAC. A survey of the slow and fast blanking of metals at ambient and high temperatures. Int. Conf. Manuf. Technol. 1967:825–51. CIRP-ASTME, Ann Arbor, Michigan.
[17] Davies R, Austin ER. Developments in high speed metal forming. The machinery publishing Co., Ltd.; 1970.
[18] Chan LT, Ong N. Design and development of an energy converter for a mechanical press and its application to high speed forming. Int J Mach Tools Manuf 2010;29:178–81.
[19] Högman B. Steel for press tools: blanking of ultra high strength steel sheet. In: 6th Int Tool Conf Use Tool Steels Exp Res. 1; 2002.
[20] Neugebauer R, Weigel P, Westkämper E, Verl A, Eicher F. Ermittlung der Einsatzpotenziale und grenzen des adiabatischen Trennen für Scherschneidlochoperationen. 2010.
[21] Winter S, Nestler M, Galiev E, Hartmann F, Psyk V, Kräusel V, et al. Adiabatic blanking: influence of clearance, impact energy, and velocity on the blanked surface. J Manuf Mater Process 2021:5. https://doi.org/10.3390/jmmp5020035.
[22] Roessig KM, Mason JJ. Adiabatic shear localization in the dynamic punch test, part II: numerical simulations. Int J Plast 1999;15:263–83. https://doi.org/10.1016/S0749-6419(98)00070-9.
[23] Winter S, Schmitz F, Clausmeyer T, Tekkaya AE, Wagner MF-X. High temperature and dynamic testing of AHSS for an analytical description of the adiabatic cutting process. J Phys Conf Ser 2016:755. https://doi.org/10.1088/1742-6596/755/1/011001.
[24] Galiev E, Winter S, Linnemann M, Winter L, Psyk V, Kräusel V. Numerical and experimental study of high-speed blanking of DC06 steel. Mater Res Proc 2023;25:27–34. https://doi.org/10.21741/9781644902417-4.
[25] Silva CMA, Rosa PAR, Atkins AG, Martins PAF. An electromagnetic testing machine for determining fracture toughness under different loading rate and superimposed pressure. J Strain Anal Eng Des 2014;49:437–44. https://doi.org/10.1177/0309324713519441.
[26] Chen ZH, Chan LC, Lee TC, Tang CY. An investigation on the formation and propagation of shear band in fine-blanking process. J Mater Process Technol 2003;138:610–4. https://doi.org/10.1016/S0924-0136(03)00141-9.
[27] Lange K. Handbook of metal forming. Society of Manufacturing Engineers; 2006.
[28] Rusinek A, Rodríguez-Martínez JA. Thermo-viscoplastic constitutive relation for aluminium alloys, modeling of negative strain rate sensitivity and viscous drag effects. Mater Des 2009;30:4377–90. https://doi.org/10.1016/j.matdes.2009.04.011.
[29] VDI-Richtlinie 2906: Schnittflächenkenngrößen. VDI-Richtlinie 2906 1994.
[30] Taylor G, Quinney H. The latent energy remaining in a metal after cold working. Proc R Soc Lond 1933;A.
[31] Hartmann C, Weiss HA, Lechner P, Volk W, Neumayer S, Fitschen JH. Measurement of strain, strain rate and crack evolution in shear cutting. J Mater Process Technol 2021;288:116872. https://doi.org/10.1016/j.jmatprotec.2020.116872.